PHYSICAL REVIEW B VOLUME 33, NUMBER 6 15 MARCH 1986

Edge magnetoplasmons in a two-dimensional electron fluid confined to a half-plane

Alexander L. Fetter
Institute of Theoretical Physics, Department of Physics, Stanford University, Stanford, California 94305-2196
(Received 4 November 1985)

The magnetoplasma modes of a two-dimensional electron fluid in a half-plane are studied with a hydrodynamic model. For general screening by parallel grounded planes, the dynamical equations are reduced to a single integral equation, whose smallest positive or negative eigenvalues correspond to anomalous edge modes. Numerical solutions are obtained by expanding in a complete set of Laguerre polynomials.

I. INTRODUCTION

A bounded two-dimensional (2D) electron fluid can support not only bulk magnetoplasma modes but also an additional edge or perimeter mode.[1–3] This new and unanticipated mode is the analog of a surface magnetoplasmon in a 3D system; it propagates along the boundary of the system and is localized there, with an amplitude that decreases rapidly toward the interior.

Theoretical models of this phenomenon have relied on two geometries: a semi-infinite half-plane[2,4,5] and a finite disk.[3,6] The former is somewhat simpler conceptually, since there is no intrinsic length scale apart from the wavelength of the mode in question. In connection with electrons on the surface of liquid He, however, the disk provides a more realistic description, because experiments rely on electrodes to create a bounded 2D electron fluid. For both models, the detailed structure of the modes depends significantly on the presence of additional grounded planes that screen the electrostatic fields.

Previous work on the half-plane has invoked a convenient approximation that replaces the problem by one that is exactly soluble.[2,4,5] This approach is not wholly satisfactory, however, for it is difficult to estimate its accuracy. As an alternative, in Sec. II of this paper I carry out an exact reduction of the coupled equations for magnetoplasma modes in a half-plane to a single integral eigenvalue equation for the induced electron density. An expansion in a complete set of Laguerre polynomials[7] yields an equivalent matrix problem (Sec. III) and numerical methods (Sec. IV) then permit a study of the convergence as more and more terms are retained. In Sec. V I consider a different geometry, in which the dielectric constant has a lateral discontinuity at the edge of the half-plane.

II. BASIC FORMULATION

The basic system of interest is a 2D electron fluid confined to a semi-infinite half-plane ($x<0$, $z=0$) and neutralized by a rigid uniform positive background with areal charge density en_0. In the undamped linearized hydrodynamic approximation, the 2D velocity $\mathbf{v}$ of the electron fluid and the perturbation n in the electron density have a harmonic time dependence $e^{-i\omega t}$. These coupled amplitudes satisfy the equation of continuity and the Euler equation

$$-i\omega n+n_0\nabla\cdot\mathbf{v}=0\ , \tag{1}$$

$$-i\omega\mathbf{v}+s^2n_0^{-1}\nabla n-em^{-1}\nabla\Phi-\omega_c\hat{\mathbf{z}}\times\mathbf{v}=0\ , \tag{2}$$

where Φ is the electrostatic potential at the plane of the charge, $\omega_c=eB/mc$ is the cyclotron frequency for motion in the applied static magnetic field, s is an effective wave speed that allows for dispersion in the propagating wave,[8] and the gradient operators involve only the x and y components.

For many purposes it is convenient[5] to introduce the 2D surface current $\mathbf{j}=-n_0e\mathbf{v}$ and the 2D conductivity tensor σ of the electron fluid

$$\sigma_{xx}=\sigma_{yy}=\frac{i\omega n_0e^2}{m(\omega^2-\omega_c^2)},\quad \sigma_{xy}=-\sigma_{yx}=\frac{\omega_c}{i\omega}\sigma_{xx}\ . \tag{3a}$$

In this way, Eq. (2) can be rewritten as

$$\mathbf{j}=-\sigma\nabla\left[\Phi-\frac{ms^2}{n_0e}n\right]. \tag{3b}$$

A combination of Eqs. (1) and (3) then yields a single dynamical equation relating the induced electron density n and the potential Φ,

$$i\omega en=\sigma_{xx}\nabla_2^2\left[\Phi-\frac{ms^2}{n_0e}n\right]+j_x\Big|_{0^-}\delta(x)\ , \tag{4}$$

where ∇_2^2 is the 2D Laplacian and the last term (proportional to the delta function) arises from the step function implicit in the conductivity tensor.

The presence of this singular term means that the electron density contains an "edge" contribution confined to the boundary of the half-plane and proportional to the component of the current flowing into the boundary, as is consistent with the equation of continuity. For the present analysis, it is convenient to make this contribution explicit, writing the full 2D density as bulk term n plus an "edge" term $n^*\delta(x)$. In this approach, Eq. (4) separates into two parts, a bulk relation (valid for $x<0$)

$$(\omega^2-\omega_c^2)en=n_0e^2m^{-1}\nabla_2^2[\Phi-ms^2(n_0e)^{-1}n]\ , \tag{5a}$$

and a boundary condition

$$i\omega e n^* = j_x\Big|_{0^-} = -\left[\sigma_{xx}\frac{\partial}{\partial x}+\sigma_{xy}\frac{\partial}{\partial y}\right]\left[\Phi-\frac{ms^2}{n_0 e}\right]\Bigg|_{0^-} , \tag{5b}$$

that relates the edge charge density to the boundary value and slope of the potential and bulk charge density as $x \to 0^-$.

These equations describe how the electrostatic fields act on the electrons, and Maxwell's equations then characterize the electrons as the self-consistent source of the fields. Specifically, I assume that the electrons are located on the surface of liquid He with dielectric constant ϵ, and that two infinite grounded planes are located symmetrically a distance h above and below the x-y plane in the vacuum and in the helium. Translational invariance along the boundary of the half-plane allows a traveling-wave solution of the form e^{iqy}, where q (which can be positive or negative according to the direction of the wave) is specified externally. It is convenient to measure all distances in units of $|q|^{-1}$, and all wave vectors in units of $|q|$. In the nonretarded (electrostatic) limit, it is not difficult to show that the potential $\Phi(x)$ at the surface of the He is determined by a nonlocal integral relation involving the total induced charge.[2,4] I introduce the quantities $N(x)$ and N^* with the dimension of a potential,

$$N(x) = \frac{4\pi e \tanh(qh)}{q(1+\epsilon)} n(x) , \tag{6a}$$

$$N^* = \frac{4\pi e \tanh(qh)}{1+\epsilon} n^* . \tag{6b}$$

The corresponding integral relation then assumes the simple form

$$\Phi(x) + \int_{-\infty}^{0} dx' K(x-x') N(x') + K(x) N^* = 0 . \tag{7}$$

Here, the variables k and x are dimensionless, and the dimensionless kernel K is given as a Fourier transform,

$$K(x) = (2\pi)^{-1} \int_{-\infty}^{\infty} dk\, e^{ikx} \bar{K}(k) , \tag{8a}$$

with

$$\bar{K}(k) = \frac{\tanh[qh(1+k^2)^{1/2}]}{(1+k^2)^{1/2}\tanh(qh)} . \tag{8b}$$

Evidently, $K(x)$ is real and even. Since a half-plane has no intrinsic geometric scale (unlike the finite disk), the single dimensionless parameter qh completely characterizes the screening by the grounded planes.

In terms of the same dimensionless variables, Eq. (5a) reduces to an ordinary differential equation,

$$\left[\frac{d^2}{dx^2}-1\right](\Omega_q^2\Phi - s^2q^2N) = (\omega^2-\Omega_c^2)N , \tag{9a}$$

along with the boundary condition

$$\left[\frac{d}{dx}+\frac{\Omega_c}{\omega}\right](\Omega_q^2\Phi - s^2q^2N)\Big|_{0^-} + (\omega^2-\Omega_c^2)N^* = 0 . \tag{9b}$$

Here Ω_q is the zero-field plasma frequency associated with a traveling wave $e^{i(qy-\omega t)}$ in an unbounded 2D electron fluid,[9,10]

$$\Omega_q^2 = \frac{4\pi n_0 e^2 q \tanh(qh)}{m(1+\epsilon)} , \tag{10a}$$

and the additional variable

$$\Omega_c = \omega_c\, \mathrm{sgn} q \tag{10b}$$

will eliminate the need for absolute-value signs.

Equations (7) and (9) constitute a pair of coupled equations for the potential $\Phi(x)$ and the density $N(x)$ valid for any value of the screening parameter qh. These two functions have different domains, however, for $N(x)$ is restricted to $x<0$, whereas the potential extends over the whole x axis. It is clear that Φ is continuous, but the presence of the edge contribution N^* implies a corresponding discontinuity in $d\Phi/dx$ at $x=0$.

Before proceeding, it is useful to consider the form of these equations for weak and strong screening. In the limit $qh \gg 1$, the grounded planes are unimportant, and the plasma frequency reduces to the familiar expression[9]

$$\Omega_q^2 = \frac{4\pi n_0 e^2 q}{m(1+\epsilon)} . \tag{11a}$$

Correspondingly, the integral kernel in Eq. (8) becomes essentially the Bessel function K_0. In this case, the approximation of replacing this exact kernel by another one with the same area and second moment[2,4,5,11] has been shown, in the nondispersive limit ($s \to 0$), to yield an approximate expression for the edge magnetoplasma modes as the roots of the quadratic equation[12]

$$3\omega^2 - 2\sqrt{2}\omega\Omega_c - 2\Omega_q^2 = 0 . \tag{11b}$$

The present numerical work provides a basis for assessing the accuracy of this prediction.

In the opposite limit ($qh \to 0$), the screening planes predominate. The bulk plasma frequency reduces to a linear dispersion relation[3]

$$\Omega_q = c_p q , \tag{12a}$$

with the propagation speed

$$c_p = [4\pi n_0 e^2 h/m(1+\epsilon)]^{1/2} . \tag{12b}$$

The kernel in Eq. (7) becomes a delta function, so that the fully screened problem is local, with $\Phi(x) = -N(x) - N^*\delta(x)$. Comparison with the general equation (4) shows that the edge charge density must vanish in this fully screened limit; otherwise higher derivatives of the delta function would be present. My numerical studies (Sec. IV) confirm the conclusion that $N^* \to 0$ as $qh \to 0$. Note that the fully screened limit is singular, in the sense that the potential now vanishes for $x>0$ (in contrast to its continuous behavior for any nonzero value of qh). Nevertheless, the limit allows for an interesting and analytic solution for all the magnetoplasma modes, including the effect of the background compressibility of the medium (the dispersive corrections of Ref. 8).

To verify this remark, observe that the "density" N now satisfies the ordinary differential equation

$$\frac{d^2N}{dx^2}=\frac{C^2q^2+\Omega_c^2-\omega^2}{C^2q^2}N\ , \tag{13}$$

where the effective wave speed is given by $C=(c_p^2+s^2)^{1/2}$. Two different types of solutions can satisfy the boundary condition in Eq. (9b) with $N^*=0$. One is the edge mode, exponentially attenuated away from the boundary, with the explicit form $N(x)=N(0)e^{\lambda x}$. The physical solution with positive λ ($=|\Omega_c|/C$ in dimensional units) has the *field-independent* frequency $\omega=-Cq$. As noted in Ref. 3, the characteristic length λ^{-1} varies inversely with the magnetic field and diverges in the zero-field limit. Thus there is no zero-field edge plasmon in the fully screened limit ($qh\rightarrow 0$), and the localization arises solely from the presence of the field. As indicated below, the situation appears to be different for finite qh, because the numerical solution (at least for selected values of qh) yields a zero-field edge mode with a frequency whose absolute value lies below the bulk value Ω_q. In addition, Eq. (13) has wavelike solutions representing bulk magnetoplasmons with spatial dependence $e^{\pm ikx}$ that are incident obliquely on the boundary and reflected specularly with amplitude $(ik+\Omega_c/\omega)\times(ik-\Omega_c/\omega)^{-1}$. In dimensional units, the corresponding frequency has the expected form[13]

$$\omega^2=C^2(k^2+q^2)+\Omega_c^2\ , \tag{14}$$

with the squared magnetoplasmon frequency increasing linearly with the squared cyclotron frequency.

To proceed with the exact solution for general values of the screening parameter qh, it is convenient to incorporate the boundary condition (9b) explicitly with a Green's function $G(x,x')$ that satisfies the differential equation

$$\left[\frac{d^2}{dx^2}-1\right]G(x,x')=-\delta(x-x') \tag{15a}$$

on the interval $-\infty<x,x'<0$, and the homogeneous boundary condition

$$\left[\left[\frac{d}{dx}+\frac{\Omega_c}{\omega}\right]G(x,x')\right]_{x=0^-}=0\ . \tag{15b}$$

It is straightforward to see that the proper solution (bounded for $x\rightarrow-\infty$) has the form

$$G(x,x')=\left[\frac{\omega-\Omega_c}{\omega+\Omega_c}\right]\gamma(x,x')+g(x,x')\ , \tag{16}$$

where the two auxiliary functions are given by

$$\gamma(x,x')=\tfrac{1}{2}e^{x+x'}\ , \tag{17a}$$

$$g(x,x')=\tfrac{1}{2}e^{-|x-x'|}\ . \tag{17b}$$

Use of Green's theorem in one dimension reduces Eq. (9) to an integral equation (valid for $x<0$),

$$\Omega_q^2\Phi(x)-s^2q^2N(x)+(\omega^2-\Omega_c^2)\int_{-\infty}^{0}dx'G(x,x')N(x')$$
$$=G(x,0)\left[\left[\frac{d}{dx}+\frac{\Omega_c}{\omega}\right](\Omega_q^2\Phi-s^2q^2N)\right]_{x=0^-}\ . \tag{18}$$

Elimination of the function Φ from Eq. (7) yields a single (still exact) integral equation for the induced electron density including both the bulk term N and the edge contribution N^*,

$$(\omega^2-\Omega_c^2)\int_{-\infty}^{0}dx'G(x,x')N(x')$$
$$-\Omega_q^2\int_{-\infty}^{0}dx'K(x,x')N(x')-s^2q^2N(x)$$
$$+[(\omega^2-\Omega_c^2)G(x,0)]-\Omega_q^2K(x,0)]N^*=0\ . \tag{19}$$

Solutions exist only for certain allowed frequencies, so that this constitutes an eigenvalue problem. Once $N(x)$ and N^* have been found, substitution back into Eq. (7), in principle, provides the corresponding potential for all x.

III. MATRIX EIGENVALUE PROBLEM

An integral eigenvalue problem can be attacked in several different ways, and here it seems simplest to expand the unknown function $N(x)$ in a complete set of orthonormal polynomials. Since the allowed domain is $[-\infty,0]$, it is natural to choose a set orthogonal on that interval, and the appearance of exponentials in Eq. (17) suggests the Laguerre polynomials.[14] With the conventional definitions, the appropriate expansion turns out to be

$$N(x)=\sum_{j=0}^{\infty}c_je^{x}L_j(-2x)\ , \tag{20}$$

where $\{c_j\}$ is a set of coefficients to be determined by substitution into Eq. (19). These polynomials satisfy the orthogonality relations

$$\int_{-\infty}^{0}dx\,e^{2x}L_i(-2x)L_j(-2x)=\tfrac{1}{2}\delta_{ij}\ , \tag{21}$$

and standard manipulations lead to an equivalent matrix eigenvalue problem for the coefficients c_j and the constant N^*,

$$\sum_{j=0}^{\infty}[(\omega^2-\Omega_c^2)G_{ij}-\Omega_q^2K_{ij}-\tfrac{1}{2}s^2q^2\delta_{ij}]c_j$$
$$+[(\omega^2-\Omega_c^2)G_i-\Omega_q^2K_i]N^*=0\ . \tag{22}$$

Here, G_{ij} is a real symmetric matrix evaluated with the Green's function from Eq. (16),

$$G_{ij}=\int_{-\infty}^{0}dx\,e^{x}\int_{-\infty}^{0}dy\,e^{y}L_i(-2x)G(x,y)L_j(-2y)\ , \tag{23a}$$

with a similar definition for the matrix elements of the kernel K_{ij}. In addition, the vector G_i is defined by

$$G_i=\int_{-\infty}^{0}dx\,e^{x}L_i(-2x)G(x,0)\ , \tag{23b}$$

and similarly for K_i.

The evaluation of the integrals involving G follows directly from Eqs. (16), (17), and the recursion relations for Laguerre polynomials.[14] In particular, it is simplest to consider separately the two functions in Eq. (17). The matrix γ_{ij} has only the single nonzero element

$$\gamma_{00}=\tfrac{1}{8}\ , \tag{24}$$

whereas g_{ij} is symmetric and tridiagonal,

$$g_{ii}=\tfrac{1}{4}, \quad g_{i,i+1}=g_{i+1,i}=-\tfrac{1}{8} . \tag{25}$$

Furthermore, the vector G_i vanishes except for the single element

$$G_0=\tfrac{1}{2}\omega(\omega+\Omega_c)^{-1} . \tag{26}$$

To treat the matrix K_{ij}, the Fourier representation in Eq. (8a) allows an explicit evaluation of the spatial integrals leaving only a single one-dimensional integral,

$$K_{j,j+l}=\frac{(-1)^l}{2\pi}\int_{-\infty}^{\infty} dk\,\bar{K}(k)(1+ik)^{l-1}(1-ik)^{-l-1} . \tag{27}$$

The substitution $k=\tan\theta$ then yields the final form

$$K_{j,j+l}=\frac{(-1)^l}{\pi}\int_0^{\pi/2} d\theta\,\bar{K}(\tan\theta)\cos(2l\theta) , \tag{28a}$$

where

$$\bar{K}(\tan\theta)=\cos\theta\coth(qh)\tanh(qh/\cos\theta) . \tag{28b}$$

This integral can be evaluated analytically for the two limiting cases of large and small qh:

$$K_{j,j+l}=\begin{cases}-[\pi(2l+1)(2l-1)]^{-1} & \text{as } qh\to\infty , \quad (29a)\\ \tfrac{1}{2}\delta_{l0} & \text{as } qh\to 0 . \quad (29b)\end{cases}$$

A similar calculation shows that

$$K_j=\frac{(-1)^j}{\pi}\int_0^{\pi/2} d\theta\,\bar{K}(\tan\theta)\frac{\cos[(2j+1)\theta]}{\cos\theta} , \tag{30}$$

with the limiting values $[\pi(2j+1)]^{-1}$ and $\frac{1}{2}$ for large and small qh, respectively. For intermediate values of qh, numerical evaluation of K_j is straightforward, and simple recursion relations then yield the corresponding matrix K_{ij}.

Inspection of Eqs. (16) and (22) shows that the frequency appears in the combinations $(\omega^2-\Omega_c^2)$ and $(\omega-\Omega_c)^2$. This unusual linear and quadratic frequency dependence in finite magnetic fields means that neither ω nor ω^2 can be considered the eigenvalue. Fortunately, the following procedure recasts the equations in the conventional form.[15] Let **c** denote the column vector of unknown coefficients (including N^*). Equation (22) then has the form $(\omega^2\underline{P}-\omega\underline{Q}-\underline{R})\mathbf{c}=0$, where $\underline{P}$, $\underline{Q}$, and $\underline{R}$ are real but asymmetric matrices. Define the additional column vector $\mathbf{d}=(\omega\underline{P}-\underline{Q})\mathbf{c}$. It is easy to see that these quantities lead to a conventional eigenvalue problem in a space with twice the original dimensions. Specifically, let **v** be a vector with elements **d** and **c**; simple manipulations then yield an equation of the form

$$\underline{A}\mathbf{v}=\omega\underline{B}\mathbf{v} , \tag{31}$$

where $\underline{A}$ and $\underline{B}$ are block matrices:

$$\underline{A}=\begin{bmatrix}\underline{0} & \underline{R}\\ \underline{1} & \underline{Q}\end{bmatrix}, \quad \underline{B}=\begin{bmatrix}\underline{1} & \underline{0}\\ \underline{0} & \underline{P}\end{bmatrix} . \tag{32}$$

Neither $\underline{A}$ nor $\underline{B}$ is symmetric, which reflects the non-self-adjoint character of the problem in finite magnetic field. Nevertheless, Eq. (31) is a generalized eigenvalue problem and can be solved by standard methods for various finite-dimensional truncations.

IV. NUMERICAL RESULTS

To investigate the convergence of the solution as the number of terms increases, the special and interesting case of an unscreened half-plane ($qh\to\infty$) was studied in detail. If the series in Eq. (20) is truncated after $p-1$ terms, the corresponding matrix equation (31) has dimension $2p\times 2p$, with $2p$ eigenvalues. Since the problem is not Hermitian, there is no guarantee that these are all real, although this turns out to be true in all cases considered. If the magnetic field is zero, the eigenvalues appear in equal and opposite pairs. As the field increases from zero ($\Omega_c>0$), all the eigenvalues increase in absolute value, apart from the negative eigenvalue closest to zero, whose absolute value instead decreases toward zero. This single mode is identified as the anomalous edge mode of the unscreened semi-infinite half-plane.

For $p=6$, 12, and 24 terms, the zero-field ratios $|\omega|/\Omega_q$ for the pair of modes with frequency closest to zero have the values 0.9003, 0.9032, and 0.9048, respectively, indicating good convergence with an increasing number of terms. Since this value is definitely less than one, the corresponding normal mode is localized near the boundary, and the characteristic decay length is of order one in these dimensionless units (and hence comparable to the wavelength of the traveling wave along the boundary). With increasing magnetic field, the mode with negative frequency becomes more localized, so that the series (20) will require more terms to provide an accurate description. Thus, for fixed small value of p, the solution eventually should worsen as the field increases. In practice, however, this effect was unimportant for the fields considered here ($\Omega_c/\Omega_q<5.0$), and the remaining calculations were performed with $p=12$. Figure 1(a) shows the field dependence of the frequency for these two modes, which are degenerate in zero field (the lower curves are labeled by the value of the parameter qh, but the upper curves are essentially independent of the screening parameter, except for very low fields). For comparison, the previous approximate quadratic relation [Eq. (11b)] is also shown (dashed). Its zero-field value of $(\frac{2}{3})^{1/2}=0.816$ is significantly lower than that found here, but it does provide a good qualitative fit to the overall magnetic field dependence.

It is interesting to consider how much of the oscillating charge in this localized edge mode is at the boundary of the half-plane. The spatial integral of the total electron density involves both the bulk and edge contributions $n(x)$ and n^*, and it is not difficult to show that the portion f_s of the total charge associated with the edge singularity is given by

$$f_s=N^*\left[\sum_j(-1)^j c_j+N^*\right]^{-1} . \tag{33}$$

The top curve of Fig. 1(b) (labeled ∞) displays the field dependence of this quantity for the unscreened negative-frequency edge mode. For small fields, most of the

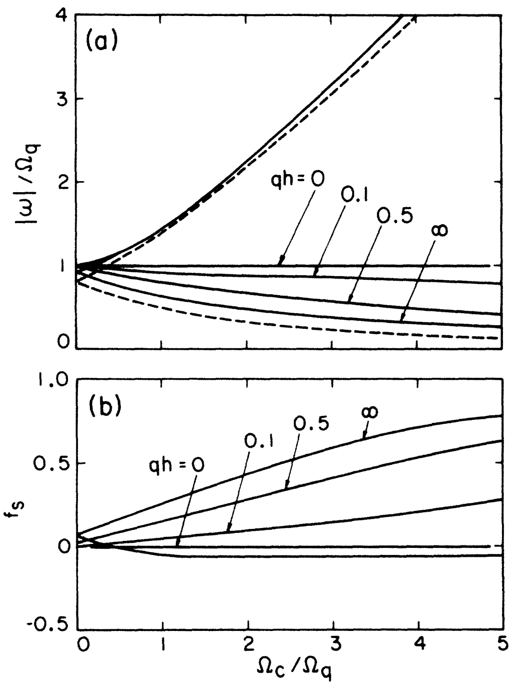

FIG. 1. (a) Numerical solution for the frequency of the smallest positive and negative magnetoplasmon modes in a half-plane. The lower solid curves describe the edge modes (with negative frequencies) for different values of the screening parameter qh. The upper solid curves describe the corresponding positive-frequency modes, which are virtually independent of the parameter qh. The dashed lines represent the previous approximation [Eq. (11b)] from Refs. 2 and 4 for an unscreened half-plane ($qh \rightarrow \infty$). (b) The portion of the total oscillating charge associated with the edge singularity at $x=0$ [Eq. (33)]. The upper four curves (labeled with the screening parameter qh) refer to the edge mode with negative frequency, and the lower curve refers to the positive-frequency mode for $qh \rightarrow \infty$ (the corresponding curves for other values of qh are essentially identical).

charge is in the bulk, but the edge contribution becomes progressively more important with increasing field. This result is consistent with the picture that the magnetic field tends to localize the mode at the boundary. In contrast, the positive-frequency mode [the bottom curve in Fig. 1(b)] has only a very small edge component, which becomes negative (out of phase) and independent of field for $\Omega_c \gtrsim \Omega_q$.

To clarify the role of the edge charge, an additional calculation was performed with $n^*=0$. As seen in Eq. (5b), this is equivalent to the simpler boundary condition $j_x|_{0^-}=0$. The resulting values of $|\omega|/\Omega_q$ for the localized edge mode increased slightly, but the dependence on the external field was very similar to that in Fig. 1(a).

Again with $p=12$, the matrix K_{ij} was evaluated numerically for $qh=0.5$ and 0.1, which represent intermediate values of the screening parameter. Figure 1(a) compares the frequency of the associated lowest normal modes with those for complete screening ($qh=0$) and the previous unscreened case ($qh \rightarrow \infty$). The positive-frequency mode is scarcely affected by the screening, apart from a small shift in the zero-field value. In contrast, increased screening reduces the field dependence of the negative-frequency mode; as noted below Eq. (13), the ratio $|\omega|/\Omega_q$ has the constant (field-independent) value 1 in the limit of perfect screening ($qh=0$), and the present numerical study confirms this behavior. It is evident in Fig. 1(b) that the portion f_s of charge associated with the boundary singularity in the localized edge mode also decreases with increased screening and vanishes entirely for perfect screening ($qh=0$).

In Ref. 4 the approximate quadratic formula in Eq. (11b) was extended to include screening. Comparison of that formula with the numerical results in Fig. 1(a) shows that the negative root [Eq. (43b) of Ref. 4] continues to provide a qualitative fit to the field dependence of the anomalous edge mode. In contrast, the positive root of the approximate formula [Eq. (43a) of Ref. 4] implies much more variation with the screening parameter qh than found here, especially at large fields. Thus that approximation fails to predict the correct field dependence of the positive-frequency modes, although it does reasonably well for the zero-field values. Similar behavior has been found for the case of edge modes in a superlattice.[5,7]

V. EDGE MODES FOR OTHER GEOMETRIES

In connection with semiconductor superlattices,[5,7] it is also interesting to consider a different geometrical configuration consisting of distinct dielectrics for $x<0$ and $x>0$ with no grounded planes; this arrangement has translational invariance along z but not x, in contrast to the preceding case of different dielectrics above and below the plane $z=0$ with horizontal grounded planes (and hence translational invariance along x but not z). The charge associated with the electron fluid in the half-plane is now to be considered "free" charge, and the usual methods of electrostatic boundary-value problems apply. Fortunately, the present case is readily treated with the method of images, and the formulation developed in Sec. II remains valid with only minor modifications.

Consider two semi-infinite dielectrics, with dielectric constants ϵ_1 for $x>0$ and ϵ_2 for $x<0$.[16] If a point charge Q is located to the left of the origin, the potential in the right-hand region is that of a charge $Q''=2\epsilon_1(\epsilon_1+\epsilon_2)^{-1}Q$ embedded at the same position in an infinite medium with dielectric constant ϵ_1. Similarly, the potential in the left-hand region is that of the original charge Q plus that of an image charge,

$$Q'=(\epsilon_2-\epsilon_1)(\epsilon_1+\epsilon_2)^{-1}Q ,$$

in an infinite medium with dielectric constant ϵ_2. More generally, in the present case of an electron fluid confined to the half-plane $x<0$ and $z=0$, the principle of superposition then yields the solution by direct integration over the charge density. In practice, it is simplest to use the three-dimensional Fourier representation of the Coulomb potential, and it is necessary to introduce two different functions to describe the resulting potential in the right and left half-spaces. For a system containing only a single semi-infinite layer, the free-charge density is given by

$$\rho_f = -e[n(x)\theta(-x)+n^*\delta(x)]e^{iqy}\delta(z) , \tag{34}$$

and a straightforward integration shows that the potential $\Phi^>$ for positive x has the form

$$\Phi^> = -\frac{4\pi e}{\epsilon_1+\epsilon_2}e^{iqy}\int_{-\infty}^{0^+}dx'\int_{-\infty}^{\infty}\frac{dk}{2\pi}e^{ik(x-x')}\frac{\exp[-|z|(k^2+q^2)^{1/2}]}{(k^2+q^2)^{1/2}}[n(x')+n^*\delta(x')] . \tag{35}$$

In contrast, the potential $\Phi^<$ for negative x contains two terms because of the direct and image charges mentioned above. This latter potential is of more direct interest, since it provides the self-consistent electrostatic force in Eq. (2).

It is again convenient to use $|q|$ in defining the same dimensionless units for distance and wave number, and to introduce the quantities [compare Eq. (6) with $qh\rightarrow\infty$]

$$N(x)=\frac{2\pi e}{\epsilon_2 q}n(x), \quad N^*=\frac{2\pi e}{\epsilon_2}n^* . \tag{36}$$

With these definitions, the integral relation corresponding to Eq. (7) has the form

$$\Phi^{>,<}(x)+\int_{-\infty}^{0}dx'K^{>,<}(x,x')N(x') + K^{>,<}(x,0)N^*=0 , \tag{37}$$

where the superscript $<$ or $>$ refers to the sign of the coordinate x. The only new feature is the detailed form of the kernel; it can still be written in the form of a Fourier integral, but the loss of translational invariance in the x direction means that it depends separately on x and x':

$$K^>(x,x')=\frac{2\epsilon_2}{\epsilon_1+\epsilon_2}\int_{-\infty}^{\infty}\frac{dk}{2\pi}e^{ik(x-x')}\bar{K}(k) , \tag{38a}$$

$$K^<(x,x')=\int_{-\infty}^{\infty}\frac{dk}{2\pi}\left[e^{ik(x-x')}+\left[\frac{\epsilon_2-\epsilon_1}{\epsilon_2+\epsilon_1}\right]e^{ik(x+x')}\right]\bar{K}(k) . \tag{38b}$$

Here, for a single layer, the function $\bar{K}(k)$ is given by [compare Eq. (8) for $qh\rightarrow\infty$]

$$\bar{K}(k)=(1+k^2)^{-1/2} . \tag{39}$$

Because of the image charge, $K^<$ contains a term involving the sum variable $x+x'$.

The remaining analysis is essentially the same as in Secs. II and III, with $K^<$ appearing throughout. In addition, Eq. (11a) is replaced by

$$\Omega_q^2=\frac{2\pi n_0 e^2 q}{m\epsilon_2} . \tag{40}$$

This quantity now characterizes the bulk 2D plasmons of a single layer in an infinite homogeneous medium with dielectric constant ϵ_2. The only substantial changes are in the matrix elements of the kernel, and Eqs. (28a) and (30) become

$$K_{jl}^< = \frac{(-1)^{j+l}}{\pi}\int_0^{\pi/2}d\theta\,\bar{K}(\tan\theta)\times\left[\cos[(j-l)2\theta]+\left[\frac{\epsilon_2-\epsilon_1}{\epsilon_2+\epsilon_1}\right]\times\cos[(j+l+1)2\theta]\right] , \tag{41a}$$

$$K_j^< = \frac{2\epsilon_2}{\epsilon_1+\epsilon_2}\frac{(-1)^j}{\pi}\int_0^{\pi/2}d\theta\,\bar{K}(\tan\theta)\frac{\cos[(2j+1)\theta]}{\cos\theta} , \tag{41b}$$

where $\bar{K}(\tan\theta)=\cos\theta$ for the case of a single layer. As noted in Sec. III, these integrals can be evaluated analytically.

To investigate the effect of the altered dielectric constants, the frequency of the smallest positive and negative modes was determined numerically for the realistic case[5,7] $\epsilon_2=13.6$ and $\epsilon_1=1$. Using $p=12$, I found the zero-field ratio $|\omega|/\Omega_q=0.998$, with the corresponding value $f_s=-0.011$ for the portion of charge in the edge singularity. As the field increased, the frequency of the positive mode was virtually indistinguishable from that in Fig. 1(a), and the associated f_s remained small and negative, attaining the constant value -0.038. In contrast, the field dependence of the negative-frequency edge mode was very similar to that labeled 0.5 in Figs. 1(a) and 1(b). Thus the presence of a large contrast in dielectric constants inhibits the formation of the edge mode but does not suppress it entirely. These conclusions confirm an independent calculation of Wu *et al.*[5]

One additional extension of this model is the case of a superlattice of semi-infinite planes spaced a distance a apart along the z axis. The presence of the neighboring charged planes produces a band of magnetoplasmons associated with different wave numbers q_z perpendicular to the planes.[5,7,17] It is convenient to introduce the function

$$S(u,v)=(\sinh u)(\cosh u-\cos v)^{-1}$$

that characterizes the screening. The quantities in Eqs. (36) and (40) acquire an extra factor $S(qa,q_z a)$, and the Fourier kernel in Eq. (39) is multiplied by

$$S(qa(k^2+1)^{1/2},q_z a)/S(qa,q_z a) .$$

Detailed study of this system requires considerable computation because the matrix elements in Eq. (41) must now be evaluated numerically. Since several specific examples have been considered in Refs. 5 and 7, this problem will not be treated here.

The present approach of using a complete set of polynomials to represent the unknown induced electron density in a half-plane appears to be efficient, especially because the resulting eigenvalue problem can be solved with standard numerical techniques. This relative simplicity should be contrasted with the (in principle) analytic solution based on the Wiener-Hopf technique,[11] which requires a displacement kernel (depending only on $x-x'$), and presumably involves a formidable numerical analysis to obtain an explicit solution for the field and screening dependence of the anomalous edge mode. The same procedure of expanding in a suitable set of polynomials also has proved effective for studying the magnetoplasmons of a 2D electron fluid confined to a disk on the surface of liquid He (Ref. 6), and it is likely to apply to other related problems.

ACKNOWLEDGMENTS

I am grateful to J. J. Quinn and J.-W. Wu for helpful discussions and correspondence, and to R. B. Laughlin for an essential suggestion. This work was supported in part by the National Science Foundation (NSF) through Grants No. DMR-81-18386 and No. DMR-84-18865.

---

[1]D. B. Mast and A. J. Dahm, Physica **126B+C**, 457 (1984).

[2]D. B. Mast, A. J. Dahm, and A. L. Fetter, Phys. Rev. Lett. **54**, 1706 (1985).

[3]D. C. Glattli, E. Y. Andrei, G. Deville, J. Poitrenaud, and F. I. B. Williams, Phys. Rev. Lett. **54**, 1710 (1985).

[4]A. L. Fetter, Phys. Rev. B **32**, 7676 (1985).

[5]J.-W. Wu, P. Hawrylak, and J. J. Quinn, Phys. Rev. Lett. **55**, 879 (1985), and unpublished.

[6]A. L. Fetter, Phys. Rev. B (to be published).

[7]J.-W. Wu, P. Hawrylak, G. Eliasson, J. J. Quinn, and A. L. Fetter (unpublished).

[8]G. Barton, Rep. Prog. Phys. **42**, 65 (1979); A. D. Boardman, in *Electromagnetic Surface Modes,* edited by A. D. Boardman (Wiley, New York, 1982), p. 1; see especially Secs. 2.1, 3.3, and 4.4.

[9]F. Stern, Phys. Rev. Lett. **18**, 546 (1967).

[10]A. V. Chaplik, Zh. Eksp. Teor. Fiz. **62**, 746 (1972) [Sov. Phys.—JETP **35**, 395 (1972)].

[11]G. F. Carrier, M. Krook, and C. E. Pearson, *Functions of a Complex Variable* (McGraw-Hill, New York, 1966), Secs. 8-1 through 8-4.

[12]Equation (11b) holds both for the simple mode boundary condition $j_x|_{0^-}=0$ used in Refs. 2 and 4, and for the more general boundary condition used in Ref. 5 and here [Eq. (5b)].

[13]N. J. M. Horing and M. Yildiz, Phys. Lett. **44A**, 386 (1973); T. Ando, A. B. Fowler, and F. Stern, Rev. Mod. Phys. **54**, 437 (1982), Sec. VI C.

[14]N. N. Lebedev, *Special Functions and their Applications* (Dover, New York, 1972), Secs. 4.17—4.24.

[15]R. B. Laughlin (private communication).

[16]See, for example, L. D. Landau and E. M. Lifshitz, *Electrodynamics of Continuous Media* (Addison-Wesley, New York, 1960), p. 40; or J. D. Jackson, *Classical Electrodynamics,* 2nd ed. (Wiley, New York, 1975), Sec. 4.4.

[17]A. L. Fetter, Ann. Phys. (N.Y.) **81**, 367 (1973); **88**, 1 (1974).